Chapter 4. Planar polarity patterns in *Drosophila*.

Before considering PCP signalling and disease mechanisms, the mutant polarity patterns and morphogenetic mechanisms of *Drosophila* will be described. The fruit-fly has been a particularly powerful model system for planar polarity largely because the adult body surface is specified within discrete imaginal discs. These epithelial sacs originate in the embryo, proliferate during the larval stages and differentiate within the pupa. The wide separation between proliferative growth and terminal differentiation contrasts with most model systems, in which these processes are intimately coupled. This study will re-examine PCP signalling and morphogenesis from the perspective of individual cells responding to distant signals, and the interactions of signal-receiving cells with their adjacent neighbours.

The first genetic analysis of planar polarity described a set of mutants with altered bristle and hair orientations [1]. Getting the hairs to align along the length of a fly's wing would seem to be a simple consequence of the mechanisms that regulate growth and differentiation, but it has turned out to be an extraordinarily complex process to analyse. As described in the initial study, the mutants show complex, invariant polarity patterns, although the wild-type pattern is relatively simple, with most bristles and hairs aligned with the direction of clonal growth. Finding a specific set of polarity-regulating genes was unexpected. Mutant wings showed complex hair orientation patterns, but the shape of the wing blade and clonal growth patterns remained unaffected. The left-wing PCP patterns are a mirror-image of the right-wing patterns, although the dorsal and ventral wing surfaces differ slightly [1], Fig. 2

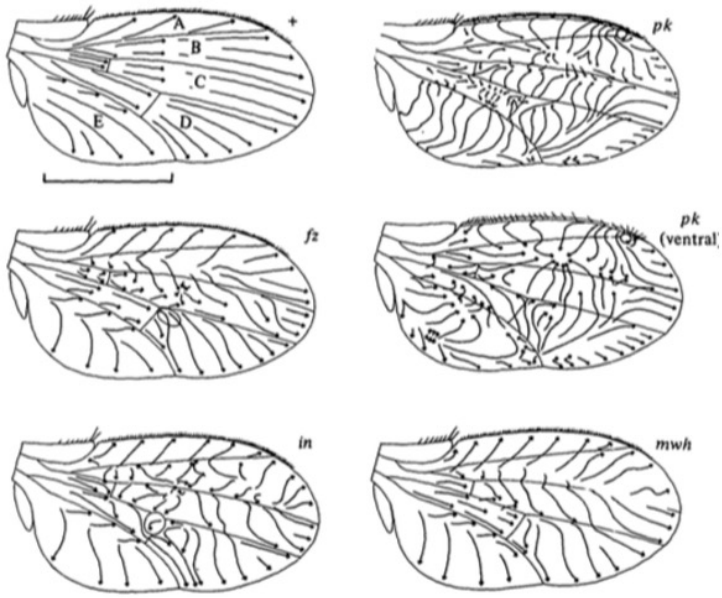

Fig. 2. Wing hair and bristle polarity: +, ***pk***, ***fz***, ***mwh*** and ***in*.** The left-wing patterns are a mirror image of the right-wing patterns (not shown), but hair orientations on the dorsal and ventral wing surfaces differ slightly (shown for *pk*). Bar = 1mm. From Gubb and Garcia-Bellido, 1982.

The PCP mutant patterns were locus-specific, rather than allele-specific, and strikingly constant from wing to wing. The genetic analysis indicated that PCP mutant phenotypes were associated with amorphic (lack of function, LOF) alleles which were viable. None gave random polarity. Surprisingly, region-specific polarity patterns were maintained in genetic

mosaics, when large clones of mutant cells were surrounded by wild-type tissue. Such regional autonomy is consistent with an underlying "pre-pattern", which could act as a template for alignment of hairs. Large mutant clones showed the typical region-specific patterns of homozygous mutant wings, and the polarity of surrounding wild-type cells was altered. These results were puzzling: if a pre-pattern were fine-grained enough to act as the template for the mutant patterns, then the wild-type tissue surrounding a mutant clone should remain keyed to this underlying pre-pattern, whatever its nature. Wild-type hairs tend to point towards *frizzled* (*fz*) mutant cells, while anterior wild-type cells reoriented towards posterior *fz* cells on the other side of the A/P compartment boundary (see below 9), Fig. 3. With smaller *fz* clones, distal (and lateral) wild-type hairs re-orient towards the mutant tissue [2]. However, the hairs of wild-type proximal cells already point towards the mutant *fz* clone, so their orientation remains unaltered.

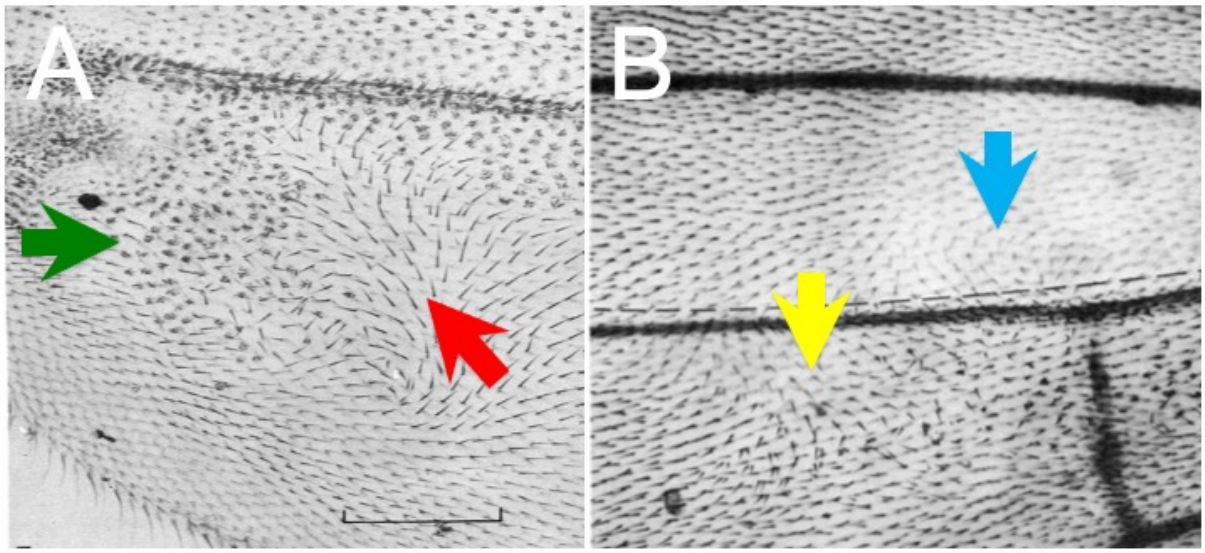

Fig. 3. Wild-type wing hairs point towards mutant *fz trc* cells. A. Hairs that are proximal to *fz trc* clones (green arrow) maintain their wild-type Pr > Dist alignment. However, wild-type hairs posterior, or distal, to *fz trc* cells are re-aligned towards the mutant clone (red arrow). **B.** Wild-type hairs in the A wing (blue arrow) may re-orient towards a *frz trc* clone in posterior wing (yellow arrow), with a domineering PCP alteration that can cross the A/P compartment boundary (dotted line). From Gubb and Garcia-Bellido, 1982.

These mosaic patterns are consistent with a morphogen sink being formed around small mutant clones, at any position along the proximo-distal (Pr/Dist) axis of the wing. The main difficulty with a morphogen gradient model, however, is that the swirling hair patterns of mutant wings do not follow the topology expected from passive diffusion. Instead, these patterns resemble the stacking flaw topologies of liquid crystals [9]. Stacking flaw topologies were first deduced from consideration of the free energy of distorting inelastic rods (splay, twist and bend) in cholesteric mesophases, calculated with respect to a rotated, helicoidal coordinate system by Frank [4] (Fig. 4). Frank's disclination topologies have since been identified in many cholesteric and nematic liquid crystalline systems, including preying mantid oothecal proteins and carbon nanotubes [5 6 7 8].

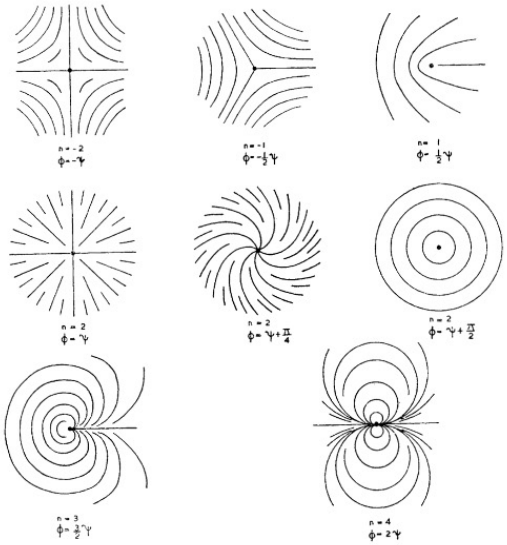

Fig. 4. Frank's predicted liquid crystalline disclinations. Similar stacking flaw topologies would be generated by sticking matchsticks, aligned in parallel with each other, to the surface of a large ball (or within the boundaries of an irregular surface) with minimal bending of the individual matchsticks. From Frank, 1958. On the surface of the globe there must be (at least) one place where the wind is not blowing.

The wing hairs in *pk*^{pk} mutants follow Frank's predicted topologies, rather than diffusion gradients [9] (Fig. 5). Similar topological disclinations are visible in many other systems, including *ft* mutant mosaics, mouse *fz6* hair patterns and myosin flux around the cortex of the embryonic blastoderm [10], see [11] (Fig. 7L) [12].

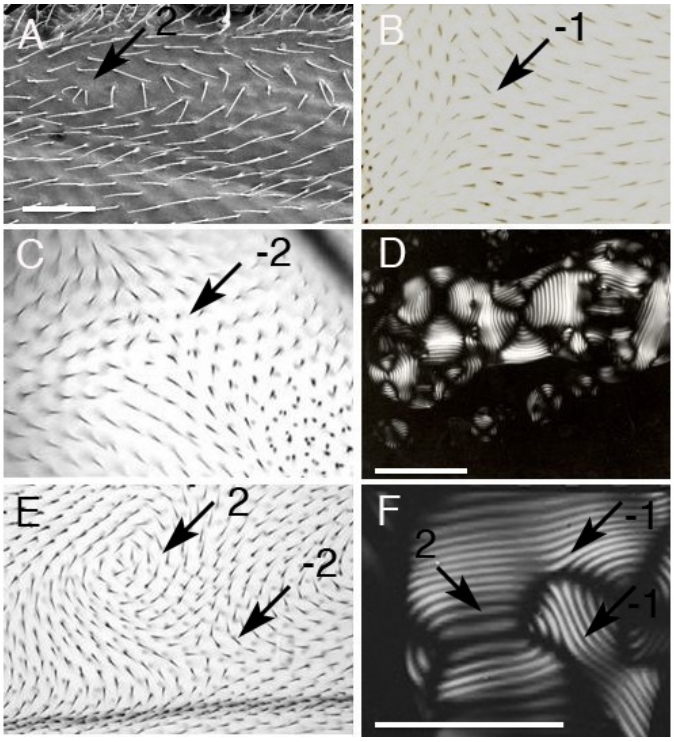

Fig. 5. Wing hair polarities in *pk*^{pk} mutants follow Frank's predicted topologies, rather than the diffusion gradients of an extracellular morphogen. Black arrows indicate disclinations,

with Frank´s topological disclinations. **A.** *pk*^{pk30}, Scanning EM. Note single cell with 3 hairs, with splayed orientations, at the centre of whorl, **n2**. **B.** Triple point disclination in *pk*^{pk30} wing blade **n-1**, phase contrast, **C.** Cruciform disclination in *pk*^{pk30} wing **n-2**, phase contrast **D.** Liquid crystalline droplet of mantid oothecal protein in phosphate buffer, light microscopy between crossed polaroid filters, white bar = 100 μ. D. Gubb, unpublished. **E.** Paired whorl **n2** and cruciform **n-2** disclinations in *da-Gal4; UAS-pk*^{sple} wing blade, phase contrast. **F.** Liquid crystalline droplet of mantid oothecal protein in phosphate buffer, **n2** whorl and **n-1** triple points, between crossed polaroid filters, white bar = 100 μ.

Later studies established that the core PCP genes encode both membrane-spanning and cytoplasmic proteins, none of which form extracellular diffusion gradients. Fz, Van Gogh (Vang, aka: Stbm), Starry night (Stan, aka: Fmi, Clsr) and Fuzzy (Fy) are transmembrane proteins; while Pk, Dishevelled (Dsh), Diego (Dgo), Fritz (Frtz), Inturned (In) and Multiple wing hairs (Mwh) are cytoplasmic, [9 13 14 15]. Strikingly, wing cells become hexagonal during the last two pupal divisions, with hair growth initiated from the distal vertex of each cell [16]. During this process, Pk, Vang, Frtz and Mwh become localised to proximal cell boundaries while Fz, Dsh and Dgo localise to the distal cell boundaries. By contrast, Stan is initially localised to both proximal and distal cell boundaries, with subsequent re-alignment [13 17 18 19]. In *stan* mutants, the wing hairs emerge from the centre of hexagonal cells [20]. However, hexagonal cell boundaries may remain aligned along the proximo-distal (Pr/Dist) axis of the wing blade, even when hair orientations are altered in PCP mutants [9 21].

Despite the orientation of wing hairs not being consistent with diffusion gradients, the tarsal joints and the eye ommatidia of PCP mutants show chiral reflections with altered cell fates [22 23 24 25]. These additional phenotypes must result from altered transmission of vectorial information. In this context, the Fz family proteins act as Wnt signalling receptors, with the Wingless (Wg) morphogen bound to exosomes and intracellular multivesicular bodies (MVBs) [26 27 28]. Thus, the orientation of bristles and hairs may give a scalar read-out of an underlying, actively transported, morphogen flux.

Intracellular gradients do transmit vectorial information along the A/P axis of the oocyte and the syncytial blastoderm [29], while, an extracellular diffusion gradient sets the embryonic dorso-ventral (D/V) axis, via the Toll (Tl) signalling pathway [30 31]. Mutations in these pathways can cause mirror-image pattern reversals like those of Mangold and Spemann's organiser. Gradients of Wg punctae are present during embryonic segmentation and near the presumptive wing tip in the L3 wing disc [32 33]. However, during larval development Wg is predominantly expressed in a narrow strip of cells around the D/V margin of the wing blade [34]. A Hh gradient is generated across the basal (Ba) epithelial surface at the A/P compartment boundary by active filopodial transport [35]. Meanwhile, gradients of the TGF-β receptor (Thick vein) and the transcriptional repressor (Spalt) are formed on apical (Ap) epithelial surfaces [36 37], see below **Chapter 29**.

Summary:

PCP mutants substitute complex, swirling patterns in place of the simple Pr > Dist alignment of bristles and hairs. These mutant patterns resemble the topological disclinations in liquid crystalline mesophases rather than extracellular diffusion gradients. Bristle and hair orientations are consistent with altered signalling through the lateral cell interfaces but can give only a scalar readout of any underlying morphogen flux. During pupal metamorphosis, the wing cells become hexagonal, with asymmetrical localisation of PCP proteins. Intracellular protein gradients have critical morphogenetic

functions and may transmit vectorial information. However, passive diffusion is insufficient to explain the regular alignment of bristles and hairs on the body surface, nor the fine-scale chiral reversals associated with PCP mutants.

References:

1. Gubb, D. & Garcia-Bellido, A. A genetic analysis of the determination of cuticular polarity during development in Drosophila melanogaster. *J. Embryol. Exp. Morphol.* **68**, 37–57 (1982).
2. Vinson, C. R. & Adler, P. N. Directional non-cell autonomy and the transmission of polarity information by the frizzled gene of Drosophila. *Nature* **329**, 549–551 (1987).
3. Gubb, D. *et al.* The balance between isoforms of the prickle LIM domain protein is critical for planar polarity in Drosophila imaginal discs. *Genes Dev.* **13**, 2315–2327 (1999).
4. Frank, F. C. I. Liquid crystals. On the theory of liquid crystals. *Discuss. Faraday Soc.* **25**, 19 (1958).
5. Rault, J. Lignes de dislocation helicoidales dans les cholesteriques. *Solid State Commun.* **9**, 1965–1969 (1971).
6. Zhang, S., Terentjev, E. M. & Donald, A. M. Stripe instability in thin films of smectic liquid-crystal polymers. *Eur. Phys. J. E* **11**, 367–374 (2003).
7. Chang, Chunrui, Lu, Kuhua, Liu, Jinghai, & Chen, Wei. Bending Deformation Mechanism and Defective Properties of Liquid Crystalline Carbon Nanotubes in Evaporating Droplets. *RSC Adv.* **1**, 468–473 (2011).
8. Shi, X. & Ma, Y. Topological structure dynamics revealing collective evolution in active nematics. *Nat. Commun.* **4**, 3013 (2013).
9. Gubb, D. *et al.* The balance between isoforms of the prickle LIM domain protein is critical for planar polarity in Drosophila imaginal discs. *Genes Dev.* **13**, 2315–2327 (1999).
10. Guo, N., Hawkins, C. & Nathans, J. Frizzled6 controls hair patterning in mice. *Proc. Natl. Acad. Sci. U. S. A.* **101**, 9277–9281 (2004).
11. Harumoto, T. *et al.* Atypical cadherins dachsous and fat control dynamics of noncentrosomal microtubules in planar cell polarity. *Dev. Cell* **19**, 389–401 (2010).
12. Streichan, S. J., Lefebvre, M. F., Noll, N., Wieschaus, E. F. & Shraiman, B. I. Global morphogenetic flow is accurately predicted by the spatial distribution of myosin motors. *eLife* **7**, (2018).
13. Strutt, D. & Strutt, H. Differential activities of the core planar polarity proteins during Drosophila wing patterning. *Dev. Biol.* **302**, 181–194 (2007).
14. Yan, J. *et al.* The *multiple-wing-hairs* gene encodes a novel GBD–FH3 domain-containing protein that functions both prior to and after wing hair initiation. *Genetics* **180**, 219 (2008).
15. Gray, R. S., Roszko, I. & Solnica-Krezel, L. Planar cell polarity: coordinating morphogenetic cell behaviors with embryonic polarity. *Dev. Cell* **21**, 120–133 (2011).
16. Wong, L. L. & Adler, P. N. Tissue polarity genes of Drosophila regulate the subcellular location for prehair initiation in pupal wing cells. *J. Cell Biol.* **123**, 209–221 (1993).
17. Tree, D. R. *et al.* Prickle mediates feedback amplification to generate asymmetric planar cell polarity signaling. *Cell* **109**, 371–81 (2002).
18. Usui, T. *et al.* Flamingo, a seven-pass transmembrane cadherin, regulates planar cell polarity under the control of Frizzled. *Cell* **98**, 585–595 (1999).

19. Classen, A. K., Anderson, K. I., Marois, E. & Eaton, S. Hexagonal packing of Drosophila wing epithelial cells by the planar cell polarity pathway. *Dev. Cell* **9**, 805–817 (2005).
20. Chae, J. *et al.* The Drosophila tissue polarity gene starry night encodes a member of the protocadherin family. *Development* **126**, 5421–5429 (1999).
21. Doyle, K., Hogan, J., Lester, M. & Collier, S. The frizzled planar cell polarity signaling pathway controls Drosophila wing topography. *Dev. Biol.* **317**, 354–367 (2008).
22. Gubb, D. Genes controlling cellular polarity in Drosophila. *Dev. Suppl* 269–277 (1993).
23. Held, L. I., Duarte, C. M. & Derakhshanian, K. Extra tarsal joints and abnormal cuticular polarities in various mutants of Drosophila melanogaster. *Rouxs Arch. Dev. Biol.* **195**, 145–157 (1986).
24. Choi, K. W., Mozer, B. & Benzer, S. Independent determination of symmetry and polarity in the Drosophila eye. *Proc. Natl. Acad. Sci. U. S. A.* **93**, 5737–5741 (1996).
25. Cooper, M. T. D. & Bray, S. J. Frizzled regulation of Notch signalling polarizes cell fate in the Drosophila eye. *Nature* **397**, 526–530 (1999).
26. Zhang, J. & Carthew, R. W. Interactions between wingless and DFz2 during Drosophila wing development. *Development* **125**, 3075–3085 (1998).
27. Wu, C. H. & Nusse, R. Ligand receptor interactions in the Wnt signaling pathway in Drosophila. *J. Biol. Chem.* **277**, 41762–41769 (2002).
28. Gross, J. C., Chaudhary, V., Bartscherer, K. & Boutros, M. Active Wnt proteins are secreted on exosomes. *Nat. Cell Biol.* **14**, 1036 (2012).
29. St. Johnston, D. & Nusslein-Volhard, C. The origin of pattern and polarity in the Drosophila embryo. *Cell* **68**, 201–219 (1992).
30. Anderson, K. V., Jurgens, G. & Nusslein-Volhard, C. Establishment of dorsal-ventral polarity in the Drosophila embryo. Genetic studies on the role of the Toll gene product. *Cell* **42**, 779–789 (1985).
31. Ligoxygakis, P., Roth, S. & Reichhart, J. M. A serpin regulates dorsal-ventral axis formation in the Drosophila embryo. *Curr. Biol.* **13**, 2097–2102 (2003).
32. Strigini, M. & Cohen, S. M. Wingless gradient formation in the Drosophila wing. *Curr. Biol.* **10**, 293–300 (2000).
33. Baeg, G.-H., Selva, E. M., Goodman, R. M., Dasgupta, R. & Perrimon, N. The Wingless morphogen gradient is established by the cooperative action of Frizzled and Heparan Sulfate Proteoglycan receptors. *Dev. Biol.* **276**, 89–100 (2004).
34. Cohen, S. M. Imaginal disc development. *Dev. Drosoph. Melanogaster* 747–841 (1993).
35. Bilioni, A. *et al.* Balancing Hedgehog, a retention and release equilibrium given by Dally, Ihog, Boi and Shifted/DmWif. *Dev. Biol.* **376**, 198–212 (2013).
36. Akiyama, T. *et al.* Dally Regulates Dpp morphogen gradient formation by stabilizing Dpp on the cell surface. *Dev. Biol.* **313**, 408–419 (2008).
37. Barrio, R., de Celis, J. F., Bolshakov, S. & Kafatos, F. C. Identification of regulatory regions driving the expression of the Drosophila spalt complex at different developmental stages. *Dev. Biol.* **215**, 33–47 (1999).